## SECED 2023 Conference

Earthquake Engineering & Dynamics for a Sustainable Future 14-15 September 2023, Cambridge, UK



# DYNAMIC SUB-STRUCTURING BASED NONLINEAR DAMPING DESIGN FOR BUILDING INTER-STORY ISOLATION SYSTEMS

Yun-Peng ZHU<sup>1</sup>, Kotaro KOJIMA<sup>2</sup>, Zi-Qiang LANG<sup>3</sup> & Bo-Yang GAO<sup>4</sup>

Abstract: Reducing inter-story drifts of building structures under earthquake ground motions is critical to increase buildings' resilience. Compared to traditional linear damping-based isolators, power-law nonlinear damping-based isolators have demonstrated the ability to achieve an overall optimal building isolation performance under ensemble earthquake ground motion records. However, current designs for nonlinearly damped building structures often require numerous complex Finite Element (FE) simulations under different types of ground motions and different values of nonlinear damping parameters. To address this challenge, the present study develops a methodology that integrates dynamic sub-structure modeling and nonlinear system frequency domain design to facilitate the optimal design of nonlinear damping for building isolation under a broad range of earthquake ground motions. To achieve this goal, firstly, a building structure is separated into sub-structures connected by isolators at the position where nonlinear dampers will be fitted. Data-driven models of these building sub-structures are identified based on a single set of force excitations and velocity responses of multiple building floors. After that, a novel equivalent linearization approach is developed to simulate the responses of the nonlinearly damped building structure. This relies on the reconstructed building model using the identified building sub-structures. Finally, the Output Frequency Response Function (OFRF) based nonlinear frequency domain design approach is applied to resolve the nonlinear damping design problem. The OFRF can produce an inherent analytical relationship between the building inter-story drifts and power-law nonlinear damping coefficients so as to be able to significantly facilitate the optimal nonlinear damping design. The application of the methodology has been demonstrated by designing a 4-story building structure. The results show that the new method can significantly increase the design efficiency and be effectively applied to the design of nonlinear building isolators under ensemble earthquake ground motion records.

#### Introduction

In practice, there has been an increasing demand for innovative seismic protection systems that can effectively mitigate the deleterious effects of earthquakes on buildings and their occupants due to the devastating impact of recent earthquakes around the world, such as the 2011 Tohoku earthquake in Japan (Mw9.1), and the 2023 Turkey-Syria earthquake (Mw7.8). Building base isolation systems and Tuned Mass Damper (TMD) systems have been widely used for seismic protection of the whole building structure (Patil and Reddy, 2012), but they are often less effective in the seismic isolation of each floor of the building. Inter-story isolation systems have been found to be a promising solution to this problem, as they can significantly reduce the transmission of seismic energy between different parts of a building (De Domenico et al., 2019).

Current implementations of inter-story isolation systems are the use of passive damping isolators, which are often less expensive and easier to use than fully active isolators such as actuators and adaptive TMD (Bolvardi et al., 2018). However, the problems with linear passive inter-story isolation are associated with compromised designs and retrofitting cost issues. For example, linear damper reduces the force transmissibility of the building system over resonant frequencies, but increases the force transmissibility over non-resonant frequencies (Guo et al., 2012) implying a compromised solution has to be considered. Compared to linear damping isolators, nonlinear damping can reduce more than 30% damping forces to allow lower retrofitting costs (De Domenico and Hajirasouliha, 2021). Moreover, recent studies (Fujita et al., 2014; Ho et al., 2018; Zhu et al., 2020) indicate that power-law nonlinear damping forces can

.

<sup>&</sup>lt;sup>1</sup> Assistant Professor, Queen Mary University of London, London, UK, yunpeng.zhu@qmul.ac.uk

<sup>&</sup>lt;sup>2</sup> Assistant Professor, Kyoto Institute of Technology, Kyoto, Japan

<sup>&</sup>lt;sup>3</sup> Professor, The University of Sheffield, Sheffield, UK

<sup>&</sup>lt;sup>4</sup> R&D Engineer, Farrat Isolevel Ltd, Manchester, UK

produce overall good building isolation performances under a broad range of earthquake ground motions, i.e. near- and far-fault ground motions with different levels of amplitudes. In the study of Ho et al. (2018), a desired building isolation performance was achieved by using a cubic nonlinear damping implemented by semi-active control of a viscous fluid damper.

Existing seismic designs of building isolation systems are often performed using complex Finite-Element (FE) simulations and similitude designs based on scaled-down experiments (Omrani et al., 2017). But these approaches are often computationally expensive and of low fidelity. Nonlinear behaviours, especially when ensemble earthquake ground motion records are taken into account, often make these building isolation design methods more prohibitive from a computational perspective. In order to circumvent the issue, dynamic sub-structuring methods can be employed. The basic idea of the dynamic sub-structuring analysis is to separate the whole system into several sub-systems connected by joint interfaces. The dynamic properties of each sub-system are studied and then combined by interface interactions to represent the dynamics of the whole system. In general, three dynamic sub-structuring methods are commonly used in practice, which are direct coupling in the physical domain (Jensen et al., 2017), component mode synthesis in the modal domain (Papadimitriou and Papadioti, 2013), and mobility analysis in the frequency domain (Mak and Su, 2003). Compared to direct coupling and component mode synthesis methods, the mobility analysis relies on Frequency Response Functions (FRFs) and is independent of system structure models, thus can be applied to resolve the cost and computational challenges of the other two methods. The mobility analysis was first developed in 1968 by Soliman and Hallam to address vibration problems between nonrigid machines and non-rigid foundation. However, the linear analysis nature makes the approach difficult to be applied to nonlinear cases. Moreover, the evaluation of sub-structure mobilities often needs multiple tests or simulations, which is impossible or difficult for the study of large scale systems such as buildings.

To address these challenges with the design of building inter-story isolation systems, a novel dynamic sub-structuring based design method for N-story building structures subject to ensemble ground motion records is developed in this study. The developed method includes (i) data-driven modelling of building sub-structures for the evaluation of mobilities, (ii) equivalent linearization (Elliott et al., 2015) of nonlinear damping forces for building simulations under ensemble ground motion records, and (iii) the Output Frequency Response Function (OFRF) (Lang et al., 2007) based design of nonlinear damping for inter-story isolations. It has been shown in our previous study (Zhu et al., 2022) that, in the dynamic sub-structuring based design of a 4-story building structure under an individual seismic ground motion, the design efficiency increases over 50% compared to the traditional design based on solving nonlinear differential equations. In the present study, the innovative dynamic sub-structuring based design method is systematically proposed for N-story building under arbitrary ground motion records. The 4-story building structure studied in (Zhu et al., 2022) will be reused to demonstrate the application of the method for inter-story isolation design under multiple near-fault earthquakes to achieve an overall optimal inter-story isolation performance.

#### The dynamic sub-structuring method

Mobility analysis of an N-story building

The N-story building system is illustrated in Figure 1 (a), where the subscribes A and C represent two sub-structures of the building,  $m_{A,i}$ ,  $i=1,...,N_a$  and  $m_{C,j}$ ,  $j=1,...,N_c$  are the masses of building floors;  $k_{A,i}$ ,  $k_B$ ,  $k_{C,j}$  and  $c_{A,i}$ ,  $c_B$ ,  $c_{C,j}$  for  $i=1,...,N_a$  and  $j=1,...,N_c$  are the linear stiffness and damping, respectively;  $\ddot{z}(t)$  is the acceleration of the ground motion, t is the continuous time;  $c_{non}$  is the additional nonlinear damping.

This N-story building system in Figure 1 (a) can be represented as a 3-layers Multiple Input Multiple Output (MIMO) vibration isolation system shown in Figure 1 (b), where

•  $f_{A,1}(t),...,f_{A,N_a}(t)$  and  $f_{C,1}(t),...,f_{C,N_a}(t)$  are input forces induced by the ground motion as

$$\begin{cases} f_{A,i}(t) = -m_{A,i}\ddot{Z}(t) & i = 1,...,N_{a} \\ f_{C,i}(t) = -m_{C,i}\ddot{Z}(t) & j = 1,...,N_{c} \end{cases}$$
 (1)

- $\gamma_{A,1}(t),...,\gamma_{A,N_a}(t)$  and  $\gamma_{C,1}(t),...,\gamma_{C,N_c}(t)$  are input velocities related to ground motion identical to the output velocities of each mass;
- p<sub>A</sub>(t), p<sub>B</sub>(t) are joint forces to layers A and B, respectively; u<sub>A</sub>(t), u<sub>B</sub>(t) are joint velocities to layers A and B related to ground motion, respectively;
- q<sub>B</sub>(t), q<sub>C</sub>(t) are joint forces to layers B and C, respectively; v<sub>B</sub>(t), v<sub>C</sub>(t) are joint velocities to layers B and C related to ground motion, respectively;

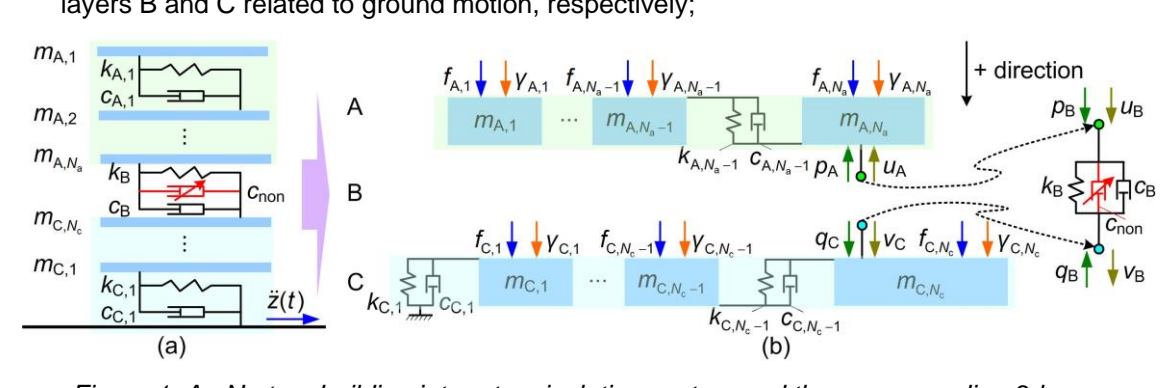


Figure 1. An N-story building inter-story isolation system and the corresponding 3-layers representation

In the case of  $c_{\text{non}} = 0$ , the building inter-story isolation system is linear. According to the mobility analysis approach (Soliman and Hallam, 1968), the velocity-force relationship of layer A can be represented in the frequency domain as

$$\mathbf{U}_{\mathsf{A}} = \mathbf{A}\mathbf{P}_{\mathsf{A}} \tag{2}$$

where

$$\mathbf{U}_{A} = \begin{bmatrix} \boldsymbol{\Gamma}_{A,1}(j\omega) \\ \vdots \\ \boldsymbol{\Gamma}_{A,N_{a}}(j\omega) \\ \boldsymbol{U}_{A}(j\omega) \end{bmatrix}, \mathbf{A} = \begin{bmatrix} \boldsymbol{A}_{1,1}(j\omega) & \cdots & \boldsymbol{A}_{1,N_{a}+1}(j\omega) \\ \vdots & \ddots & \vdots \\ \boldsymbol{A}_{N_{a}+1,1}(j\omega) & \cdots & \boldsymbol{A}_{N_{a}+1,N_{a}+1}(j\omega) \end{bmatrix}, \mathbf{P}_{A} = \begin{bmatrix} \boldsymbol{F}_{A,1}(j\omega) \\ \vdots \\ \boldsymbol{F}_{A,N_{a}}(j\omega) \\ \boldsymbol{P}_{A}(j\omega) \end{bmatrix}$$

$$(3)$$

In (3),  $\Gamma_{A,1}(j\omega)$ ,  $\Gamma_{A,2}(j\omega)$ ,... are the spectra of the input velocities  $\gamma_{A,1}(t)$ ,  $\gamma_{A,2}(t)$ ,...,  $\omega$  is the frequency (rad/s);  $U_A(j\omega)$  is the spectra of the joint output velocity  $u_A(t)$  to layer A;  $F_{A,1}(j\omega)$ ,  $F_{A,2}(j\omega)$ ,... are the spectra of the input forces  $f_{A,1}(t)$ ,  $f_{A,2}(t)$ ,...;  $P_A(j\omega)$  is the spectra of the joint output force  $p_A(t)$  to layer A.

The four-pole relationship of layer B (Molloy, 1957) can be written as

$$\begin{cases} P_{\rm B}(j\omega) = B_{\rm l,1}(j\omega)Q_{\rm B}(j\omega) + B_{\rm l,2}(j\omega)V_{\rm B}(j\omega) \\ U_{\rm B}(j\omega) = B_{\rm 2,1}(j\omega)Q_{\rm B}(j\omega) + B_{\rm 2,2}(j\omega)V_{\rm B}(j\omega) \end{cases}$$
(4)

where  $P_{\rm B}(j\omega)$  and  $Q_{\rm B}(j\omega)$  are the spectra of the joint forces  $p_{\rm B}(t)$  and  $q_{\rm B}(t)$  to layer B, respectively;  $U_{\rm B}(j\omega)$  and  $V_{\rm B}(j\omega)$  are the spectra of the joint velocities  $u_{\rm B}(t)$  and  $v_{\rm B}(t)$  to layer B, respectively;  $B_{i,j}(j\omega)$ , i,j=1,2 are complex functions of  $\omega$ .

For layer C, velocity-force relationship in the frequency domain is similar to that of layer A, and is obtained as

$$V_{C} = CQ_{C} \tag{5}$$

where

$$\mathbf{V}_{C} = \begin{bmatrix} \Gamma_{C,1}(j\omega) \\ \vdots \\ \Gamma_{C,N_{c}}(j\omega) \\ V_{C}(j\omega) \end{bmatrix}, \mathbf{C} = \begin{bmatrix} C_{1,1}(j\omega) & \cdots & C_{1,N_{c}+1}(j\omega) \\ \vdots & \ddots & \vdots \\ C_{N_{c}+1,1}(j\omega) & \cdots & C_{N_{c}+1,N_{c}+1}(j\omega) \end{bmatrix}, \mathbf{Q}_{C} = \begin{bmatrix} F_{C,1}(j\omega) \\ \vdots \\ F_{C,N_{c}}(j\omega) \\ Q_{C}(j\omega) \end{bmatrix}$$

$$(6)$$

In (6),  $\Gamma_{\text{C,1}}(j\omega)$ ,  $\Gamma_{\text{C,2}}(j\omega)$ ,... are the spectra of the input velocities  $\gamma_{\text{C,1}}(t)$ ,  $\gamma_{\text{C,2}}(t)$ ,...;  $V_{\text{C}}(j\omega)$  is the spectra of the joint output velocity  $v_{\text{C}}(t)$  to layer C;  $F_{\text{C,1}}(j\omega)$ ,  $F_{\text{C,2}}(j\omega)$ ,... are the spectra of the input forces  $f_{\text{C,1}}(t)$ ,  $f_{\text{C,2}}(t)$ ,...;  $Q_{\text{C}}(j\omega)$  is the spectra of the joint output force  $q_{\text{C}}(t)$  to layer C.

The interaction between the interfaces of layers A and B, as well as layers B and C, are described by

$$-P_{A}(j\omega) + P_{B}(j\omega) = 0 \text{ and } U_{A}(j\omega) = -U_{B}(j\omega)$$
 (7)

$$-Q_{R}(j\omega) + Q_{C}(j\omega) = 0 \text{ and } V_{R}(j\omega) = V_{C}(j\omega)$$
(8)

Therefore, based on the relationships of (2), (4), (5), (7) and (8), the linear output force  $Q_B(j\omega)$  can be evaluated as (Appendix A):

$$Q_{\mathrm{B}}(j\omega) = -\frac{1}{M(j\omega)} \left[ S(j\omega) \sum_{j=1}^{N_{\mathrm{c}}} C_{N_{\mathrm{c}}+1,j}(j\omega) F_{\mathrm{C},j}(j\omega) + \sum_{i=1}^{N_{\mathrm{a}}} A_{N_{\mathrm{a}}+1,i}(j\omega) F_{A,i}(j\omega) \right]$$
(9)

where

$$\begin{cases} M(j\omega) = B_{2,1}(j\omega) + B_{1,1}(j\omega)A_{N_a+1,N_a+1}(j\omega) + S(j\omega)C_{N_c+1,N_c+1}(j\omega) \\ S(j\omega) = B_{2,2}(j\omega) + B_{1,2}(j\omega)A_{N_a+1,N_a+1}(j\omega) \end{cases}$$

As a result, when  $Q_B(j\omega)$  is obtained, output force  $Q_C(j\omega)$  and velocity  $V_C(j\omega)$  to layer C can be evaluated by  $Q_C(j\omega) = Q_B(j\omega)$  and  $\mathbf{V}_C = \mathbf{CQ}_C$ ; according to the four-pole relationship (4),  $V_B(j\omega) = V_C(j\omega)$ , and the joint force can be obtained as  $P_B(j\omega) = B_{1,1}(j\omega)Q_B(j\omega) + B_{1,2}(j\omega)V_B(j\omega)$ . Thus, output force  $P_A(j\omega)$  and velocity  $U_A(j\omega)$  to layer A can be evaluated by  $P_A(j\omega) = P_B(j\omega)$  and  $\mathbf{U}_A = \mathbf{AP}_A$ . The corresponding time domain results can be directly obtained by the inverse Fourier Transform of the evaluated spectra.

Evaluation of mobility matrices from sub-structure models

It can be seen from the above analysis that, given the mobility matrices  $\bf A$  and  $\bf C$ , as well as  $B_{i,j}(j\omega)$ , i,j=1,2, the output responses of a linear building inter-story isolation system can be calculated in the frequency domain, rather than solving a set of complex differential equations.

Consider the linear inter-story isolator is composed of a spring and a damper, then (Soliman and Hallam, 1968)

$$B_{1,1}(j\omega) = 1, B_{1,2}(j\omega) = 0, B_{2,1}(j\omega) = \frac{j\omega}{k_{\rm B} + c_{\rm B}j\omega}, B_{2,2}(j\omega) = 1$$
 (10)

In practice, conventional evaluation of mobility matrices **A** and **C** based on sub-structure modal analysis often requires multiple tests to evaluate the whole mobility matrices. In order to resolve this challenge, the present study proposes to identify a multiple inputs single output ARX (AutoRegression with eXogenous input) model for each output velocity with the data used for sub-structure modelling obtained from one physical simulation of the linear building system under a sufficiently excited ground motion.

For example, in the velocity-force relationship (2), the velocity  $\Gamma_{\Delta}$ , (j $\omega$ ) can be represented as

$$\Gamma_{A,1}(j\omega) = A_{1,1}(j\omega)F_{A,1}(j\omega) + \dots + A_{1,N_{c}}(j\omega)F_{A,N_{c}}(j\omega) + A_{1,N_{c}+1}(j\omega)P_{A}(j\omega)$$
(11)

which indicates that the output and joint output velocities can be represented by a linear system with input and joint output forces. This linear system can be represented by MISO (Multiple

Inputs Single Output) ARX models as

$$\gamma_{A,1}(k) = \theta_{\gamma,1}\gamma_{A,1}(k-1) + \dots + \theta_{\gamma,n_{\gamma}}\gamma_{A,1}(k-n_{\gamma}) + \sum_{i=1}^{N_a} [\theta_{f_{i},0}f_{A,i}(k) + \dots + \theta_{f_{i},n_{i,j}}f_{A,i}(k-n_{f,i})] + \theta_{p,0}p_{A}(k) + \dots + \theta_{p,n_{n}}p_{A}(k-n_{p})$$
(12)

where k is the discrete time; n are maximum time delays and  $\theta$  are model coefficients.

Then, the associated mobility between  $\gamma_{A,1}(t)$  and  $f_{A,1}(t),...,f_{A,N}(t),p_A(t)$  can be obtained as

$$A_{l,i}(j\omega) = \frac{\theta_{f_i,0} + \sum_{k=1}^{n_{l,i}} \theta_{f_i,k} \exp(-jk\omega\Delta t)}{1 - \sum_{k=1}^{n_{l,i}} \theta_{v,k} \exp(-jk\omega\Delta t)}, A_{l,N_a+1}(j\omega) = \frac{\theta_{\rho,0} + \sum_{k=1}^{n_{p}} \theta_{\rho,k} \exp(-jk\omega\Delta t)}{1 - \sum_{k=1}^{n_{v}} \theta_{v,k} \exp(-jk\omega\Delta t)}$$
(13)

where  $i = 1,...,N_a$ ,  $\Delta t$  is the sampling time of the ARX model.

As a result, other entries for the mobility matrix  $\bf A$ , as well as the mobility matrix  $\bf C$ , can be evaluated following the same procedure. The corresponding MISO ARX models can be identified using the Regularized Least Square (RLS) method (Filipovic, 2015). Considering the input forces  $f_{\rm A,1}(t),\ldots,f_{\rm A,N_a}(t)$  are specified by designers,  $p_{\rm A}(t)$  and concerned velocities used for MISO ARX modelling are obtained from a numerical simulation of the linear building system.

## **Equivalent linearization for mobility analyses**

In general, mobility analysis can only be applied to linear systems. Therefore, the nonlinear damped building inter-story isolation system cannot be directly investigated by using the mobility analysis method.

In order to resolve this issue, an equivalent linearization approach was proposed in (Elliott et al., 2015; Zhu et al., 2022) to find a linear damping  $c_{\rm eq}$  producing equivalent damping force to the nonlinear damping  $c_{\rm non}$ . In this case, the four-pole parameters of layer B can be represented as

$$B_{1,1}(j\omega) = 1, B_{1,2}(j\omega) = 0, B_{2,1}(j\omega) = \frac{j\omega}{k_{\rm B} + (c_{\rm B} + c_{\rm eq})j\omega}, B_{2,2}(j\omega) = 1$$
 (14)

Denote the relative velocity  $w(t) = u_B(t) - v_B(t)$ , the additional power-law nonlinear damping force can be represented as

$$f_{\text{non}}(t) = \sum_{r=2}^{R} c_{\text{non},r} w(t)^{r}, R \in \mathbb{Z}^{+}$$
 (15)

where  $c_{non,r}$  are nonlinear damping coefficients. The equivalent damping force is

$$f_{\rm eq}(t) = c_{\rm eq} w(t) \tag{16}$$

The equivalence of the damping force is obtained by an error minimization approach (Elliott et al., 2015; Zhu et al., 2022). The Mean Square Error (MSE) between the nonlinear damping force and the equivalent linear damping force is

$$\eta_{\text{MSE}} = E\{[f_{\text{non}}(t) - f_{\text{eq}}(t)]^2\}$$
(17)

where  $E\{.\}$  represents the mean value.

The equivalent linear damping can be obtained by minimizing the MSE (17) as (Zhu et al., 2022)

$$c_{\text{eq}} = \frac{E\left\{\sum_{r=2}^{R} c_{\text{non},r} w(t)^{r+1}\right\}}{E\left\{w(t)^{2}\right\}}$$
(18)

In (18), it is worth noting that the relative velocity w(t) calculated from the equivalent linear building system is also dependent on the equivalent linear damping  $c_{\rm eq}$ . Thus, the equivalent linear damping can be evaluated by solving

$$J(c_{eq}) = c_{eq} - \frac{E\left\{\sum_{r=2}^{R} c_{\text{non},r} w(t)^{r+1}\right\}}{E\left\{w(t)^{2}\right\}} = 0$$
 (19)

using a bisection searching algorithm introduced in (Zhu et al., 2022).

## Nonlinear damping design in the frequency domain

#### The OFRF representation

The OFRF representation reveals an analytical relationship between the output spectrum of nonlinear systems and the parameters which define system nonlinearities, so that can be used to facilitate the optimal nonlinear damping design (Lang et al., 2007). Consider the building inter-story isolator is implemented by a power-law nonlinear damping (15), under the condition that the building linear dynamics are fixed, the OFRF representation of the system output response can be expressed as a polynomial function

$$Y(j\omega) = \sum_{(j_1, \dots, j_S) \in J} \varphi_{j_1, \dots, j_S}(j\omega) \xi_1^{j_1} \dots \xi_S^{j_S}$$
(20)

where  $Y(j\omega)$  represents an output spectrum of the building isolation system such as the output force  $Q_{\rm B}(j\omega)$  or the velocity  $V_{\rm C}(j\omega)$ ;  $\{\xi_1,\ldots,\xi_S\}\subseteq\{c_{{\rm non},2},\ldots,c_{{\rm non},R}\}$  are nonlinear damping coefficients for design;  $\phi_{j_1,\ldots,j_S}(j\omega)$  are the coefficients of the OFRF;  ${\bf J}$  is a set of integers.

Assume there are M polynomial terms in the OFRF representation (20) and  $N \ge M$  sets of output spectra  $Y^{(n)}(j\omega)$ , n = 1,...,N have been determined using the mobility analysis under different nonlinear damping parameters over a space of design defined by end users. Denote

$$\mathbf{Y} = \begin{bmatrix} \mathbf{I} \\ \mathbf{Y}^{(n)}(\mathbf{j}\omega) \\ \mathbf{I} \end{bmatrix}, \mathbf{E} = \begin{bmatrix} \mathbf{I} & \mathbf{I} & \mathbf{I} \\ - & \boldsymbol{\xi}_{1}^{(n)j_{1}} \cdots \boldsymbol{\xi}_{S}^{(n)j_{S}} & - \\ \mathbf{I} & \mathbf{I} & \mathbf{I} \end{bmatrix}, \boldsymbol{\Phi} = \begin{bmatrix} \mathbf{I} \\ \boldsymbol{\varphi}_{j_{1},\cdots,j_{S}}(\mathbf{j}\omega) \\ \mathbf{I} & \mathbf{I} \end{bmatrix}$$
(21)

such that the OFRF representation (20) can be written into a matrix form as  $\mathbf{Y} = \mathbf{E}\mathbf{\Phi}$ , where the coefficients  $\mathbf{\Phi}$  can be evaluated by using the Least Squares (LS) method as

$$\mathbf{\Phi} = (\mathbf{E}^{\mathsf{T}}\mathbf{E})^{-1}\mathbf{E}^{\mathsf{T}}\mathbf{Y} \tag{22}$$

Nonlinear damping design

Considering the linear properties of a building isolation system is fixed. The design of nonlinear damping for building inter-story isolator is summarized as follows.

#### Step 1: Set up the OFRF representations

Determine a maximum monomial order in the OFRF representation (20) of the output spectrum subject to a ground motion. The OFRF representing the overall performance of the building isolation system under all concerned ground motions for design can be derived to perform the nonlinear damping design under ensemble earthquake ground motion records.

## Step 2: Determine OFRF representations based on equivalent linearization

Assuming there are M monomials in an OFRF representation. Select  $N \ge M$  different sets of nonlinear damping parameter values over the design space, and calculate the output spectra of the nonlinearly damped building isolation system by using the equivalent linearization approach. The OFRF representations can be determined by using the LS algorithm (22).

#### Step 3: The OFRF based system design

The objective function for the design of nonlinear damping can be formulated based on the OFRF representation, so as to find the optimised nonlinear damping values by solving an optimization problem: Find the nonlinear damping values  $\boldsymbol{\xi} = \{\xi_1, \dots, \xi_S\}$  to solve the optimization problem  $\min_{\boldsymbol{\xi}} \eta(\boldsymbol{\xi})$  under the constraint  $\xi_{s,\min} \leq \xi_s \leq \xi_{s,\max}; s=1,\dots,S$ , where  $\eta(\boldsymbol{\xi})$  is the objective function for the design.

## Case study - Design of nonlinearly damped inter-story isolation system

Consider a 4-story building system in Figure 2 (a) with a nonlinear damper  $f_{\text{non}}(t) = c_{\text{non,3}}w(t)^3$  located between the 2nd and the 3rd floor, where (Zhu et al., 2022)

$$\begin{split} & m_{\text{C},\text{1}} = 8.95 \times 10^5 \text{ kg}, \ m_{\text{C},\text{2}} = 8.98 \times 10^5 \text{ kg}, \ m_{\text{A},\text{2}} = 8.70 \times 10^5 \text{ kg}, \ m_{\text{A},\text{1}} = 5.76 \times 10^5 \text{ kg}, \\ & k_{\text{C},\text{1}} = 3.92 \times 10^7 \text{ N/m}, \ k_{\text{C},\text{2}} = 3.09 \times 10^7 \text{ N/m}, \ k_{\text{B}} = 2.67 \times 10^7 \text{ N/m}, \ k_{\text{A},\text{1}} = 1.94 \times 10^7 \text{ N/m}, \\ & c_{\text{C},\text{1}} = 6.86 \times 10^5 \text{ Ns/m}, \ c_{\text{C},\text{2}} = 5.41 \times 10^5 \text{ Ns/m}, \ c_{\text{B}} = 4.67 \times 10^5 \text{ Ns/m}, \ c_{\text{A},\text{1}} = 3.4 \times 10^5 \text{ Ns/m}, \end{split}$$

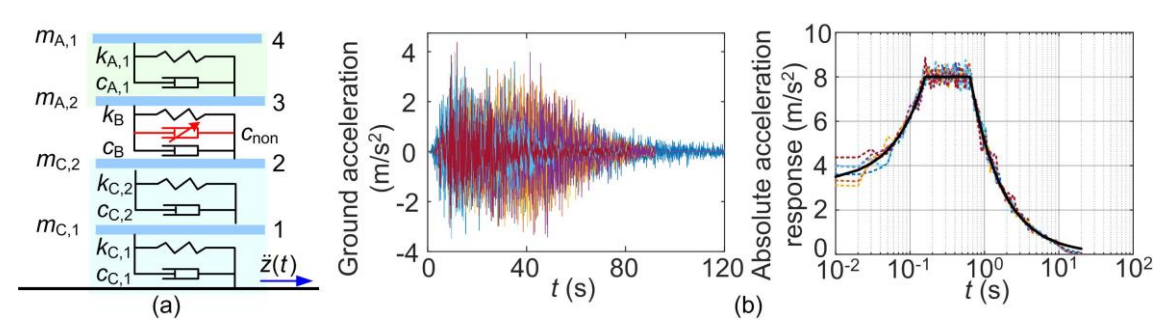


Figure 2. (a) The 4-story building model, (b) The 7 concerned ground motions for design (Black line: The safety-limit design spectrum)

In this case study, optimal nonlinear damping design is conducted under a set of Safety-Limit Response-Spectrum Compatible (SLRSC) ground motions illustrated in Figure 2 (b). These ground motions are known as Kokuji waves covering different lengths with 4 random phases and 3 phases of El Centro NS, Taft NS (EERL, 1971) and Hachinohe NS (Tsuchida et al., 1969) according to the safety-limit level at engineering bedrock surface in Japanese seismic design code and standard building law in Japan (NILIM, et al., 2020).

The optimization problem is to find the values of the system damping parameter  $c_{\text{non,3}}$  to solve the optimization problem

$$\eta(c_{\text{non,3}}) = \min_{c_{\text{non,3}}} E_{\text{sum}}^{(\text{average})} = \min_{c_{\text{non,3}}} \frac{1}{R} \sum_{r=1}^{R} (E_{1,2}^{(r)} + E_{3,4}^{(r)})$$
(23)

subject to  $c_{\text{non},3} \in [1,100] \times 10^7 \text{ Ns}^3/\text{m}^3$ , where  $E_{\text{sum}}^{\text{(average)}}$  is the average sum of the power of the inter-story drift between floors 1 and 2 and floors 3 and 4. In this example,  $E_{2,3}^{(r)}$  is not considered. The super-scribe (r) represents the r th design wave and the inter-story energy  $E_{i,i}^{(r)}$  are defined as

$$E_{i,j}^{(r)} = \sum_{k=0}^{K} d_{i,j}^{(r)} (k\Delta t)^2 \Delta t, (i,j) = (1,2), (2,3), (3,4)$$
(24)

with  $d_{i,j}^{(r)}$ , (i,j) = (1,2),(2,3),(3,4) being the inter-story drift between *i*th and *j*th floors.

The dynamic sub-structuring based design of nonlinear damping is conducted as follows.

#### Step 1: Set up the OFRF representations

According to Parseval's Theorem, the inter-story drift energy  $E_{i,j}$  is the sum of the square of the inter-story drift in the frequency domain. Thus, the OFRF representation of  $E_{1,2} + E_{3,4}$  under an individual Kokuji wave can be written as (Zhu et al., 2022)

$$E_{12}^{(r)} + E_{34}^{(r)} = \varphi_0^{(r)}(j\omega) + \varphi_1^{(r)}(j\omega)c_{\text{non}3} + \dots + \varphi_{10}^{(r)}(j\omega)c_{\text{non}3}^{10}$$
(25)

with the sufficient large order of the OFRF taken as 10. The average OFRF representation of the inter-story energy under the seven Kokuji waves is obtained as

$$E_{\text{sum}}^{(\text{average})} = \frac{1}{7} \sum_{r=1}^{7} \varphi_0^{(r)}(j\omega) + \frac{1}{7} \sum_{r=1}^{7} \varphi_1^{(r)}(j\omega) c_{\text{non},3} + \dots + \frac{1}{7} \sum_{r=1}^{7} \varphi_{10}^{(r)}(j\omega) c_{\text{non},3}^{10}$$
(26)

#### Step 2: Determine OFRF representations based on equivalent linearization

ARX models of the two sub-structures of the 4-story building structure are identified from sufficiently random excitation forces that cover all magnitudes and frequencies of the seismic loadings of concern. Selected mobility matrices evaluated from these ARX models are shown in Figure 3 (a) and compared with theoretical results obtained from the differential equations.

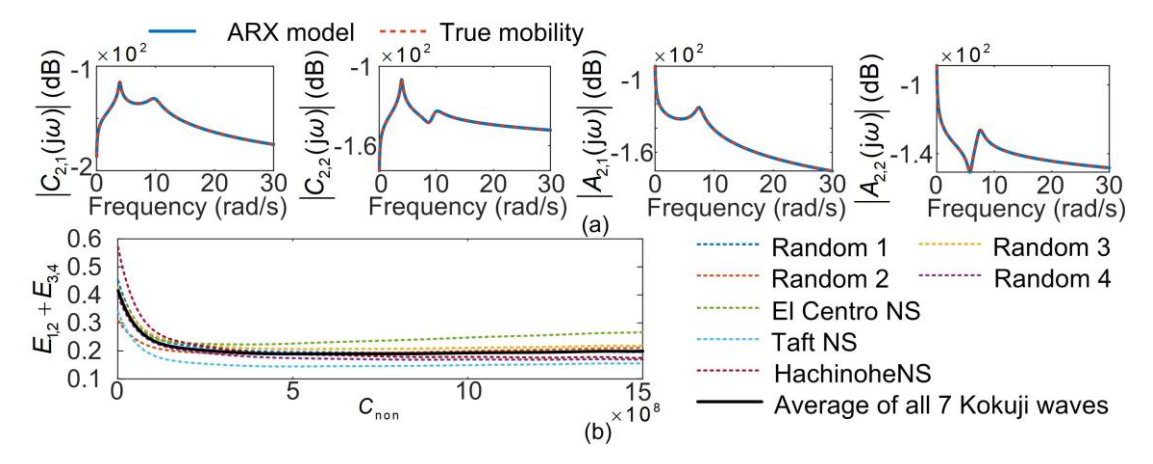


Figure 3. (a) The mobility matrices identified from the sub-structure ARX models, (b) The OFRF representations of inter-story energies

After that, equivalent linearization approach is applied to simulate the building system with nonlinear damper. Building output responses under N = 21 different nonlinear damping values are calculated to evaluate the OFRF of the average inter-story energy as shown in Figure 3 (b).

#### Step 3: The OFRF based system design

By solving the optimization problem (23), the minimum average inter-story energy of the 4-story building system is obtained at  $c_{\text{non 3}} = 5.11 \times 10^8 \text{ Ns}^3/\text{m}^3$ .

In order to validate the design result, three recorded high-amplitude near-fault pulse-like ground motions during 1995 Hyogoken-Nanbu earthquake and 2016 Kumamoto earthquake in Japan are applied, which are the JMA Kobe NS component during 1995 Hyogoken-Nanbu earthquake, Mashikimachi (KiK-net) EW component and Nishiharamurakomori (Kumamoto prefecture) EW component during 2016 Kumamoto earthquake as shown in Figure 4 (NIED, 2019).

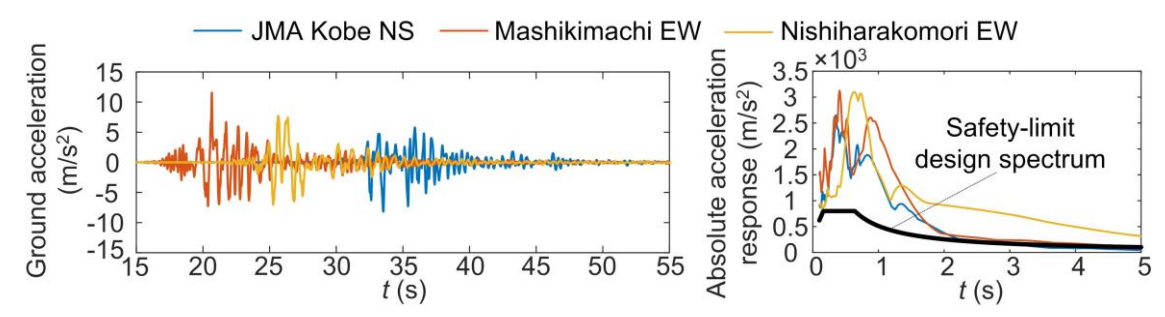


Figure 4. Waveforms and response spectra of the three recorded near-fault ground motions

Table 1 shows the inter-story drift energy  $E_{\rm sum}$  of the 4-story building model with the optimal  $c_{\rm non,3}$  under the three near-fault pulse-like ground motions evaluated by differential equation simulations. From Table 1, the optimal  $c_{\rm non,3}$  for the Kokuji waves can reduce  $E_{\rm sum}$  under the JMA Kobe NS and Mashikimachi EW, achieving the same optimal performance as in the case under the corresponding individual ground motion. On the other hand, the optimal  $c_{\rm non,3}$  for the Kokuji waves cannot reduce  $E_{\rm sum}$  under the Nishiharamurakomori EW efficiently compared with the ideal performance. However, the design result can reduce  $E_{\rm sum}$  under the Nishiharamurakomori EW by 60%. Therefore, overall, the designed nonlinear damping  $c_{\rm non,3}$  can significantly reduce the inter-story drift energy of the building system under the near-fault ground motions with much higher amplitudes.

	JMA Kobe NS	Mashikimachi EW	Nishiharamurakomori EW
$c_{\text{non,3}} = 0$	0.167	0.490	4.114
$c_{\text{non,3}} = 5.11 \times 10^8$	0.087	0.258	1.599
$c_{\text{non,3}} = 1.22 \times 10^8$	0.090	-	-
$c_{\text{non,3}} = 1.02 \times 10^8$	-	0.257	-
$c_{\text{non,3}} = 0.51 \times 10^8$	-	-	1.276

Table 1 Inter-story energy of the 4-story building with designed  $c_{\text{non,3}}$  and optimized  $c_{\text{non,3}}$  for individual waves of JMA Kobe NS, Mashikimachi EW and Nishiharakomori EW

#### Conclusions

Designing nonlinearly damped inter-story building isolation systems through many runs of FE simulations or numerally solving differential equations is computationally expensive and complicated. Dynamic sub-structuring method based on mobility analysis can overcome these complexities, but has limitations in studying nonlinear systems and requires dedicated physical tests or numerical simulations on system substructures. To address these issues, a novel dynamic sub-structuring based design method integrating data-driven modelling of sub-structures, equivalent linearization of nonlinear damping, and the OFRF based design has been developed. The efficiency and effectiveness of this new approach have been demonstrated by a case study on the design of a 4-story nonlinearly damped building isolation system. The results indicate that the optimal damping parameters designed under ensemble ground motions can provide desirable inter-story isolation performance under near-fault seismic with both the designed and higher amplitudes. The proposed methodology has the potential to enhance the efficiency of the isolator designs for complex building systems and leverage the development of nonlinear vibration isolation designs for a broad range of engineering applications.

## Appendix A

In the 3-layers model of the *N*-story building system, layers A and C are connected by layer B. From equation (2), the joint output velocity is

$$U_{A}(j\omega) = A_{N_{a}+1,1}(j\omega)F_{A,1}(j\omega) + \dots + A_{N_{a}+1,N_{a}}(j\omega)F_{A,N_{a}}(j\omega) + A_{N_{a}+1,N_{a}+1}(j\omega)P_{A}(j\omega)$$
(A1)

Considering the interaction  $-P_{\rm A}(j\omega) + P_{\rm B}(j\omega) = 0$  and  $U_{\rm A}(j\omega) = -U_{\rm B}(j\omega)$  as well as the four-pole relationship (4), there is

$$-[B_{2,1}(j\omega)Q_{B}(j\omega) + B_{2,2}(j\omega)V_{B}(j\omega)] = A_{N_{a}+1,1}(j\omega)F_{A,1}(j\omega) + \dots + A_{N_{a}+1,N_{a}}(j\omega)F_{A,N_{a}}(j\omega) + A_{N_{a}+1,N_{a}+1}(j\omega)[B_{1,1}(j\omega)Q_{B}(j\omega) + B_{1,2}(j\omega)V_{B}(j\omega)]$$
(A2)

Similarly, by using  $-Q_{\rm R}(j\omega) + Q_{\rm C}(j\omega) = 0$  and  $V_{\rm R}(j\omega) = V_{\rm C}(j\omega)$ , from equation (5), there is

$$V_{\rm B}(j\omega) = C_{N,+1,1}(j\omega)F_{\rm C,1}(j\omega) + \dots + C_{N,+1,N}(j\omega)F_{\rm C,N}(j\omega) + C_{N,+1,N,+1}(j\omega)Q_{\rm B}(j\omega) \tag{A3}$$

Substituting (A3) into (A2), yields

$$\begin{split} -B_{2,1}(j\omega)Q_{B}(j\omega) - B_{2,2}(j\omega)C_{N_{c}+1,N_{c}+1}(j\omega)Q_{B}(j\omega) - B_{2,2}(j\omega)\sum_{j=1}^{N_{c}}C_{N_{c}+1,j}(j\omega)F_{C,j}(j\omega) \\ &= \sum_{i=1}^{N_{a}}A_{N_{a}+1,i}(j\omega)F_{A,i}(j\omega) + A_{N_{a}+1,N_{a}+1}(j\omega)B_{1,1}(j\omega)Q_{B}(j\omega) \\ &+ A_{N_{a}+1,N_{a}+1}(j\omega)B_{1,2}(j\omega)\sum_{j=1}^{N_{c}}C_{N_{c}+1,j}(j\omega)F_{C,j}(j\omega) + A_{N_{a}+1,N_{a}+1}(j\omega)B_{1,2}(j\omega)C_{N_{c}+1,N_{c}+1}(j\omega)Q_{B}(j\omega) \end{split}$$
(A4)

Therefore,  $Q_{\rm B}({\rm j}\omega)$  can be solved as (9)

### Acknowledgement

The ground motions used in this paper were provided by Japan Meteorological Agency, KiK-net (National Research Institute for Earth Science and Disaster Resilience) and Kumamoto prefecture.

#### References

- Patil SJ and Reddy GR (2012). State of art review-base isolation systems for structures. *International journal of emerging technology and advanced engineering*, 2(7): 438-453.
- De Domenico D, Ricciardi G and Takewaki I (2019). Design strategies of viscous dampers for seismic protection of building structures: a review. *Soil dynamics and earthquake engineering*, 118: 144-165.
- Bolvardi V, Pei S, van de Lindt, JW and Dolan JD (2018). Direct displacement design of tall cross laminated timber platform buildings with inter-story isolation. *Engineering Structures*, 167: 740-749.
- Guo PF, Lang ZQ and Peng ZK (2012). Analysis and design of the force and displacement transmissibility of nonlinear viscous damper based vibration isolation systems. *Nonlinear Dynamics*, *67*, 2671-2687.
- De Domenico D and Hajirasouliha I (2021). Multi-level performance-based design optimisation of steel frames with nonlinear viscous dampers. *Bulletin of Earthquake Engineering*, 19(12): 5015-5049.
- Fujita K, Kasagi M, Lang ZQ, Guo PF and Takewaki, I. (2014). Optimal placement and design of nonlinear dampers for building structures in the frequency domain. *Earthquakes and Structures*, 7(6): 1025-1044.
- Ho C, Zhu YP, Lang ZQ, Billings SA, Kohiyama M and Wakayama S (2018). Nonlinear damping based semi-active building isolation system. *Journal of Sound and Vibration*, 424: 302-317.
- Zhu YP, Lang ZQ, Kawanishi Y and Kohiyama M (2020). Semi-actively implemented non-linear damping for building isolation under seismic loadings. *Frontiers in Built Environment*, 6: 19.
- Omrani S, Garcia-Hansen V, Capra B and Drogemuller R (2017). Natural ventilation in multistorey buildings: Design process and review of evaluation tools. *Building and Environment*, 116: 182-194.
- Jensen H., Araya VA, Muñoz AD and Valdebenito MA (2017). A physical domain-based substructuring as a framework for dynamic modeling and reanalysis of systems. *Computer Methods in Applied Mechanics and Engineering*, 326: 656-678.
- Papadimitriou C and Papadioti DC (2013). Component mode synthesis techniques for finite element model updating. *Computers & structures*, 126: 15-28.
- Mak CM and Su JX (2003). A study of the effect of floor mobility on structure-borne sound power transmission. *Building and Environment*, 38(3): 443-455.
- Soliman JI and Hallam MG (1968). Vibration isolation between non-rigid machines and non-rigid foundations. *Journal of Sound and Vibration*, 8(2): 329-351.
- Elliott SJ, Tehrani MG and Langley RS (2015). Nonlinear damping and quasi-linear modelling. *Philosophical Transactions of the Royal Society A: Mathematical, Physical and Engineering Sciences*, 373(2051): 20140402.
- Lang ZQ, Billings SA, Yue R and Li J (2007). Output frequency response function of nonlinear Volterra systems. *Automatica*, 43(5): 805-816.
- Zhu YP, Lang ZQ, Fujita K and Takewaki I (2022). The Design of Nonlinear Damped Building Isolation Systems by Using Mobility Analysis. *Frontiers in Built Environment*, 177.
- Molloy CT (1957). Use of Four-Pole Parameters in Vibration Calculations. *The Journal of the Acoustical Society of America*, 29(7): 842-853.
- Filipovic VZ (2015). Recursive identification of multivariable ARX models in the presence of a priori information: robustness and regularization. *Signal processing*, 116: 68-77.
- NIED 2019, K-NET & KiK-net data, *National Research Institute for Earth Science and Disaster Resilience*, https://www.kyoshin.bosai.go.jp/
- Earthquake Engineering Research Laboratory (EERL) (1971). Strong motion earthquake accelerograms, digitized and plotted data, Volume II corrected accelerograms and integrated ground velocity and displacement curves; Part A Accelerograms IIA001 through IIA020. California Institute of Technology.
- Tsuchida H, Kurata E and Sudo K (1969) Strong-motion earthquake records on the 1968 Tokachi-oki earthquake and its aftershocks. *Technical Note of The Port and Harbour Research Institute Ministry of Transport. Japan*, No. 80, June 1969.
- National Institute for Land and Infrastructure Management (NILIM) et al. (2020). Commentary on Structural Regulations of the Building Standard Law of Japan, 2020 edition, Official Gazette Co-operation of Japan. (in Japanese)